Applied Soft Computing 14 (2014) 594–602

Contents lists available at ScienceDirect

Applied Soft Computing

journal homepage: www.elsevier.com/locate/asoc

Review article

A fuzzy logical controller for traffic load parameter with priority-based rate in wireless multimedia sensor networks

Young-Long Chen*, Hung-Pin Lai

Department of Computer Science and Information Engineering, National Taichung University of Science and Technology, No. 129, Sec. 3, Sanmin Road, Taichung 404, Taiwan

ARTICLE INFO

Article history:
Received 24 May 2012
Received in revised form 24 May 2013
Accepted 7 August 2013
Available online 13 September 2013

Keywords:
Wireless multimedia sensor networks
Quality of service
Exponential weight
Fuzzy logical controller

ABSTRACT

In *wireless multimedia sensor networks* (WMSNs), sensor nodes use different types of sensors to gather different types of data. In multimedia applications, it is necessary to provide reliable and fair protocols in order to meet specific requirements of *quality of service* (QoS) demands in regard to these different types of data. To prolong the system lifetime of WMSNs, it is necessary to perform adjustments to the transmission rate and to mitigate network congestion. In previous works investigating WMSNs, *exponential weighted priority-based rate control* (EWPBRC) schemes with *traffic load parameter* (TLP) schemes in WMSNs were used to control congestion by adjusting transmission rates relative to various data types. However, when the TLP is fixed, a large change in data transmission causes a significant difference between input transmission rate and the estimated output transmission rate of each sensor node. This study proposes a novel *fuzzy logical controller* (FLC) pertaining to TLP schemes with an EWPBRC that estimates the output transmission rate of the parent node and then assigns a suitable transmission rate based on the traffic load of each child node, with attention paid to the different amounts of data being transmitted. Simulation results show that the performance of our proposed scheme has a better transmission rate as compared to PBRC: the delay and loss probability are reduced. In addition, our proposed scheme can effectively control different transmission data types insofar as achieving the QoS requirements of a system while decreasing network resource consumption.

Contents

1. Introduction

Rapid technological advances in wireless communication systems, low power digital electronics, small scale energy supplies, micro-microprocessors and low power radio technologies now enable low-power multi-functional sensor devices to detect and react to changes in their surrounding environments. These sensor devices are equipped with a small battery, a tiny micro-processor and a set of transducers that are used to acquire information which reflects these changes in the surrounding environment of the sensor node. The emergence of low power and minute wireless sensor devices has led to intensive research in the last decade which, in turn, has led to the development of *wireless sensor networks* (WSNs) [1].

A *wireless sensor network* (WSN) consists of one or more sink nodes and numerous sensor nodes scattered in a wireless field, which collaborate with each other to accomplish certain tasks. Specifically, a wireless sensor network is a physical device which

* Corresponding author. Tel.: +886 4 22196621; fax: +886 4 22196341.
E-mail address: ylchen66@nutc.edu.tw (Y.-L. Chen).

1568-4946/$ – see front matter © 2013 Elsevier B.V. All rights reserved.
http://dx.doi.org/10.1016/j.asoc.2013.08.001

integrates information from sensor computing and wireless communication processing. Mutual propagation of data is sent from neighboring nodes to the *base station* (BS). A *wireless multimedia sensor network* (WMSN) [2] is an extended application of WSNs such that the sensor can be equipped with a multimedia device, e.g., a miniaturized microphone, battery or video transceiver; therefore, WMSNs have the capability to transmit multimedia data such as still images, video and audio streams, along with the ability to monitor data. Resource constraints on WMSNs include: energy, memory, bandwidth, buffer size and processing capability. Since multimedia data transmission requires high transmission rates and the ability to process massive amounts of data, the high data transmission rate common to WMSNs often causes congestion. This, in turn, deteriorates the *quality of service* (QoS) of multimedia applications.

With regard to WSNs, limited power, bandwidth, high density network and large scale deployments underscore some challenges to the management and design of WSNs. As such, these challenges demand energy awareness and protocol designs at all layers of the networking protocol. Efficient use of sensor energy resources is the main design consideration in developing protocols and algorithms with regard to sensor networks and has dominated most of the research pertaining to WSNs. Furthermore, WMSNs, in real-time applications, require strict constraints on both delay and throughput in order to report the time-critical data to the processing sink within certain time limits and bandwidth requirements without loss. Hence, energy awareness for sensor networks with different layers requires an efficient utilization of network resources, as well as effective access to sensor readings [3].

In WMSNs, disseminating packets are used to carry information and transmit data via a hop-by-hop process. The transmission priorities of heterogeneous WMSNs differ between real-time transmission and non-real-time transmission. Real-time transmission has major constraints such as delay and bandwidth jitter, but is more tolerant to packet losses. Transmission rates do not need to be controlled in real-time transmission, which has the highest priority, but non-real-time transmission uses an active queue management scheme [4] to allocate transmission rate. Studies of factors affecting QoS in network transmission, including packet loss probability, delay and throughput, indicate that packet loss probability and delay can usually be mitigated.

In network transmissions, QoS enables stable and predictable data transmission service in order to satisfy network users' requirements. Internet data flows, such as those for e-commerce, multimedia data transmission and massive file downloads, usually require massive transmissions of burst data which then cause congestion [5]; notably, increased bandwidth cannot solve the resulting insufficiencies with regard to network resources. The *internet engineering task force* (IETF) defines a service differentiation model [6] to guarantee the QoS of end-to-end transmission.

Energy consumption is also an important issue in regard to wireless networks. Chamodrakas and Martakos [7] proposed a network selection method based on a modified fuzzy version of the *technique for order preference by similarity to the ideal solution* (TOPSIS) with regard to QoS and energy consumption. Additionally, Chen et al. [8] proposed scheme utilizes local information regarding feedback control commands for power adjustments in wireless cellular networks. In [9], the authors proposed a *fuzzy logical controller* (FLC) to manage rates and achieve selective power control for *code division multiple access* (CDMA) systems. In the literature [10], FLC combined with power control vis-a-vis window-based transmission rate management was proposed in a multimedia CDMA cellular system. The FLC is used to make adaptive rate adjustments and monitor power control in regard to transmission rate. Here, two input values, *signal-to-interference ratio* and *error-to-error change*, are used to adjust transmission rate control and power control. Furthermore, some studies [11,12] proposed using the FLC power control to select a suitable channel using non-linear time variant characteristics.

A model based on transmission priority has been proposed to mitigate network transmission congestion in a WMSN. In terms of transmission rate, the fixed *traffic load parameter* (TLP) scheme was used for adjustment purposes. In the TLP [13] scheme with *exponential weighted priority-based rate control* (EWPBRC), the transmission data exhibit massive variations and a large error between input transmission rate and estimated transmission rate for each sensor node, resulting in inconsistent network resource allocation. The traffic load parameter was a fixed value to yield such that the delay and loss probability for the WMSN is increased.

This paper proposes a new scheme in which we use FLC to regulate traffic load parameters based on EWPBRC for controlling the transmission rate of each sensor node, in order to avoid resource waste caused by excessive adjustments of the transmission rate. However, a transmission rate that is too low can cause excessive adjustments, leading to too much delay. The proposed scheme has two FLC input variables: transmission rate error and error change. Via the FLC, the traffic load parameter is adjusted in order to optimize the transmission rate of each sensor node.

The remainder of this paper is organized as follows: Section 2 consists of an investigation of related research regarding WMSNs in transmission congestion control; Section 3 provides details regarding the proposed scheme for improving transmission; Section 4 contains the simulation results; and Section 5 offers our conclusions.

2. Related works

This section describes the effects of transmission congestion on network resources and QoS. Currently, traditional *transmission control protocol* (TCP) is widely used in computer networks; TCP uses packet confirmation to provide reliable transmission. The congestion control architecture used to meet the QoS requirement of WMSNs in different data types is also discussed.

For data transmission in WSNs, the network transmission model layer must be coordinated. Different layers have different control topics. During data transmission, the *media access control* layer (MAC), RTS/CTS and ACK mechanisms enable transmission to the sensor node of each mobile. In WMSNs, the MAC layer gathers the transmitted information and measures queuing delay in order to compute the transmission rate [14].

Transmission rate congestion control in WSNs has been studied extensively. Congestion leads to massive packet loss; consequently, the re-transmission of lost packets causes further congestion and wastes network resources, while decreasing the reliability of data detection and collection. Congestion in WSNs [5] may be embodied by node-level congestion or link-level congestion. In node-level congestion, when the packet-arrival rate exceeds the packet service rate at each sensor node, buffer overflow increases packet loss when the node transmits data. Link-level congestion occurs in wireless transmissions when the nodes use the same channel, such as in *carrier sense multiple access with collision detection* (CSMA/CD). When multiple active nodes use the same channel, the resulting collision is detected [15] and the node in the collision must sends out a congestion message to the entire network. At this moment, all network nodes must cease transmission and enter a waiting state.

There are two approaches to control congestion: network resource management and traffic control [5]. Network resource management mitigates congestion via the increase of network resources. This is undertaken, for instance, through an enhancement of bandwidth where congestion is slowed. When this method is used, the precise adjustment of network resources is required in

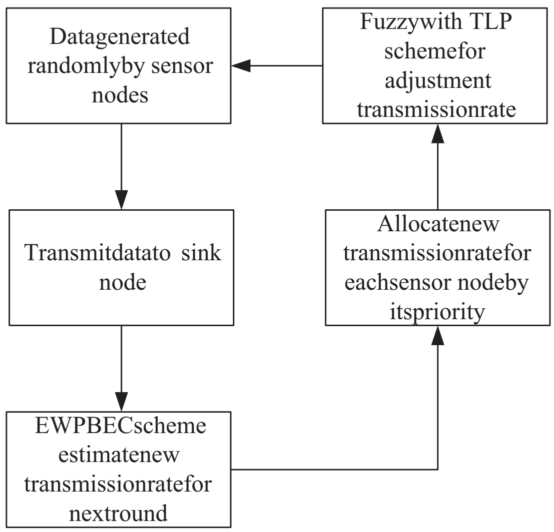

Fig. 1. Simulation phase for our proposed scheme.

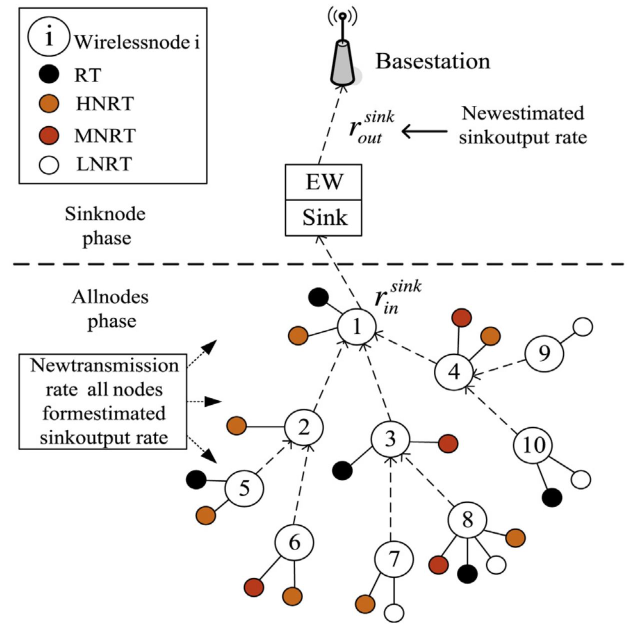

Fig. 2. A traffic class model for WMSNs.

order to avoid resource overloading. For transmission control, the traffic control approach is used to adjust the source node or intermediate node of congestion in order to conserve network resources and increase those resources' effectiveness. Most of the current congestion control protocols belong to this type. There are two methods with which to control traffic: *end-to-end* and *hop-by-hop*. The end-to-end method can be used to precisely adjust the rate of each source node; however, the response is slow and the *round-trip time* (RTT) of the packet needs to be considered. Hop-by-hop has a faster response time in regard to congestion control as it is chiefly used under the MAC protocol; however, adjusting the forwarding rate of the packet for the intermediate node is difficult.

3. The FLC for TLP based on EWPBRC

In this section, our proposed scheme combines a priority-based rate with FLC to regulate TLPs for the improvement of transmission performance. In [13], Yaghmaee and Adjeroh proposed the EWPBRC scheme to control the transmission rate of the sink node. Then, the transmission rate of the sink node will follow the exponential weighted priority-based rate control scheme with the fixed TLP [13] to yield a larger delay and loss probability for a WMSN. To improve the performance of WMSNs, we propose a new scheme such that the *FLC for traffic load parameter* (FTLP) is based on EWPBRC. Hence, we can obtain the optimum TLP and transmission rate for all child nodes and diminish the delay time and loss probability for WMSNs. In the simulation phase, we set up the sensor node traffic classes in advance according to their function. The transmission data are generated randomly and transmit data to the sink node according to their transmission path. We use the EWPBRC scheme to estimate new transmission rates for the next round; then, the new transmission rate allocates each sensor node according to its priority. In the end, the FLC combined with the TLP scheme for adjusting transmission rate is shown in Fig. 1.

3.1. A heterogeneous traffic classes model

Fig. 2 shows the simulation model, symbols and scheme [13] of the proposed and simulated WMSN environmental hypothesis. There are ten nodes, one sink node and the *base station* (BS). We defined four different types of data with regard to amount and priority class among the ten nodes, which are: *rapid traffic* of a real-time (RT) transmission type and three types of non-real-time transmission. These are: *high-priority non-real-time* (HNRT), *medium-priority non-real-time* (MNRT) and *low-priority non-real-time* (LNRT). In the sink node phase, Yaghmaee and Adjeroh [13] proposed an EWPBRC scheme with the fixed TLP for transmission rate adjustment. Here, a weight parameter was used to adjust the transmission rate of the sink node. Then, the traffic class and geographical location priority are based on distributing to all nodes in all nodes phases, as shown in Fig. 2.

3.2. Rate adjustment scheme

In the rate adjustment schemes, each node i is divided into one of two different priority classes: *traffic class priority* (P^i_{TRC}) and *geographic location priority* (P^i_{GEO}). SP^i_j denotes the traffic source priority j in sensor node i; the priority order SP^i_j of the source priority can be manually set up with service differentiation, and the higher the SP^i_j value, the higher the traffic class. P^i_{TRC} is the sum SP^i_j of the traffic class of the source data of node i. It is represented as:

$$P^i_{\mathrm{TRC}} = \sum_j SP^i_j \tag{1}$$

where j is traffic class; j belongs to {RT, HNRT, MNRT, LNRT}.

The following is the transmission rate calculation for our proposed scheme to be FTLP with EWPBRC, which can be divided into three phases: the EWPBRC for the sink output transmission rate phase, the new output transmission for the child nodes phase and computing the new output transmission rate for each parent node in the FTLP phase.

Step 1: EWPBRC for the sink output transmission rate adjustment phase

From the average transmission rate $\bar{r}^{\mathrm{sink}}_{\mathrm{out}}(n)$ and $r^{\mathrm{sink}}_{\mathrm{out}}(n)$ at time instant n, we can obtain the $r^{\mathrm{sink}}_{\mathrm{out}}(n+1)$ output transmission rate at time instant $n+1$:

$$r^{\mathrm{sink}}_{\mathrm{out}}(n+1) = \bar{r}^{\mathrm{sink}}_{\mathrm{out}}(n)\cdot(1-\lambda) + \lambda\cdot r^{\mathrm{sink}}_{\mathrm{out}}(n) \tag{2}$$

where λ is constant, $0 \le \lambda \le 1$ and λ is 0.5 for all schemes.

Step 2: The new output transmission rate for the child node phase

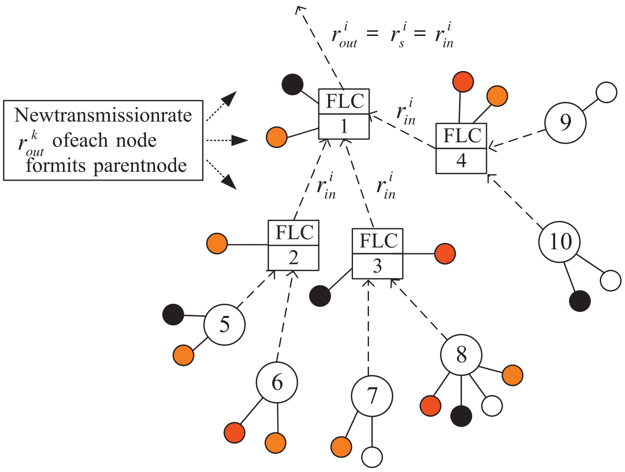

Fig. 3. FTLP traffic class model for WMSNs.

In WMSNs, based on functionality, different types of sensor nodes will be equipped and a node will be deployed at a related geographical location according to the different levels of importance. In data transmission, based on the geographical location, an appropriate priority and transmission rate will be given. P^i_{GEO} is the geographical location priority of node i. The total priority P^i of node i is related to traffic class priority P^i_{TRC} and geographic location priority P^i_{GEO}, defined as:

$$P^i = P^i_{\text{TRC}} \cdot P^i_{\text{GEO}} \tag{3}$$

$C(i)$ is the set of child nodes of node i; the global priority GP^i of each node i is calculated as follows: in the simulation, if there are no other child nodes in node i, its global priority will be equal to its total P^i value:

$$GP^i = \sum_{k \in C(i)} GP^k + P^i \tag{4}$$

GP^{sink} is the sum of the global priorities of the sink node, $C(\text{Sink})$ is the set of all the child nodes with the sink as their parent and GP^{sink} is the sum of the priorities of all the nodes:

$$GP^{\text{sink}} = \sum_{k \in C(\text{Sink})} GP^k \tag{5}$$

To calculate the output transmission rate r^i_{out} of node i, r^i_{out} is calculated on the basis of the distribution of the output transmission rate $r^{\text{sink}}_{\text{out}}$ from the sink node to node i according to the proportion of the global priority of child node GP^i to the global priority of sink node GP^{sink}:

$$r^i_{\text{out}} = r^{\text{sink}}_{\text{out}} \cdot \frac{GP^i}{GP^{\text{sink}}} \tag{6}$$

Step 3: Computing a new output transmission rate for each parent node in the FTLP phase

In this phase, we propose an FTLP to regulate the TLP and obtain the optimal transmission rate of each sensor node. Then, the transmission rate of the parent node will follow the TLP scheme [13] to achieve a transmission rate distribution on each sensor node, as shown in Fig. 3.

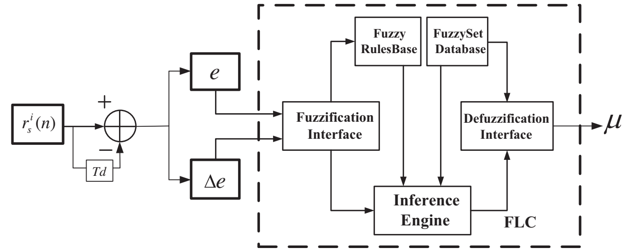

Fig. 4. Block diagram of FTLP rate control.

We define r^i_{in} as the input transmission rate of node i, which is obtained through the summation of the r^k_{out} of the connected child nodes; r^i_{in} is calculated as follows:

$$r^i_{\text{in}} = \sum_{k \in C(i)} r^k_{\text{out}} \tag{7}$$

where $C(i)$ is the set of node i, and r^k_{out} is represented as the output rate of the kth child of parent node i.

r^i_{out} is node i's output transmission rate and is calculated as:

$$r^i_{\text{out}} = r^i_s + r^i_{\text{in}} \tag{8}$$

where r^i_s is node i measures data from itself.

Δr^i is the transmission rate difference of node i and is given by:

$$\Delta r^i = \mu \cdot r^i_{\text{out}} - r^i_{\text{in}} \tag{9}$$

where the TLP μ is the defuzzification output value. In Section 3.3, we use FLC to obtain the optimum TLP μ.

Each parent node i generates a new transmission rate to be distributed among all the child node k output transmission rates; this is calculated as:

$$r^k_{\text{out}} = r^k_{\text{out}} + \Delta r^i \cdot \frac{GP^k}{GP^i} \tag{10}$$

3.3. Our proposed FLC model

The FLC system consists of five components: a fuzzificaion interface, a fuzzy set database, a rule base, an inference engine and a defuzzification interface, as shown in Fig. 4. The function of each component is as follows [14]. The fuzzification interface converts each input value into suitable linguistic variables which can be viewed as terms of fuzzy sets. These fuzzy sets are used for partitioning the continuous domains of the FLS input/output values into a small number of overlapping regions using linguistic terms. The fuzzy set database manages the uncertainty and vagueness associated with entities, attributes and relationships. Notably, this can be implemented in a relational database model. The fuzzy rule base consists of the expert knowledge of the application domain and the attendant control targets; fuzzy data is used as a rule base by which to control the system. The interface engine is a decision-making mechanism of the FLC; it controls fuzzy variables and infers fuzzy rules. The defuzzification interface consists of deriving a single crisp value usable for a concrete real-world control action from inferred fuzzy output values. In this paper, the defuzzification output is computed using the centroid-defuzzifier method [15].

In Fig. 4, we also evaluated the effects the transmission TLP μ on delay and loss probability. We have proposed the FTLP scheme with EWPBRC such that FLC can regulate TLP and control the output transmission rate of each node.

As shown in Fig. 4, we have used FLC to determine TLP μ, where error e and error change Δe are used as two input variables in the FLC. $e(n)$ is the error between $r^i_s(n)$ and $r^i_s(n-1)$ at time instant n:

$$e(n) = r^i_s(n) - r^i_s(n-1) \tag{11}$$

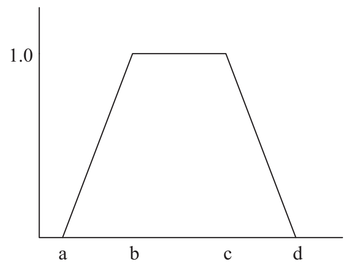

Fig. 5. Trapezoidal membership functions.

where the r_s^i is node *i* measuring data from itself and *Td* is the unit delay.

$\Delta e(n)$ is the error change of two continuous times of *e* in time instant *n*:

$$\Delta e(n) = e(n) - e(n-1) \tag{12}$$

Fuzzy sets and memberships function values provide a possible model for inexact concepts and subjective judgments for all types of estimation. Fuzzy set *A* in a universe of discourse *X* is defined as the following set of pairs:

$$A = \{(\mu_A(x), x) : x \in X\} \tag{13}$$

where $\mu_A : X \to [0, 1]$ is mapping such that the membership function of the fuzzy set *A* and $\mu_A(x)$ is called the degree of membership value of $x \in X$ in the fuzzy set *A*.

Fig. 5 illustrates the seven trapezoidal membership functions which have been used. There associated membership functions are the commonly used trapezoidal functions. The trapezoidal membership function is specified by four parameters {*a*, *b*, *c*, *d*} as follows:

$$Trapezoid\ (x : a, b, c, d) = \left\{ \begin{array}{ll} 0 & x < a \\ \dfrac{x-a}{b-a} & a \le x < b \\ 1 & b \le x < a \\ \dfrac{d-x}{b-c} & c \le x < d \\ 0 & x > d \end{array} \right\} \tag{14}$$

There are seven fuzzy linguistic variables: two-input values are *large positive* (LP), *medium positive* (MP), *small positive* (SP), *zero* (ZE), *small negative* (SN), *medium negative* (MN) and *large negative* (LN). Output values contain seven membership functions, namely: *extremely low* (EL), *very low* (VL), *low* (L), *medium* (M), *high* (H), *very high* (VH) and *extremely high* (EH) as shown in Fig. 6.

The fuzzy rules are based on the relationship between oscillations in dimension of the solution vector during the iterations and speed of convergence. The rules for convergence [12] is that control increment has the same sign as *e* and Δe. Nevertheless, we use the FLC in this system that the overshoot is drastically reduced and oscillation is effectively excluded. The rate of convergence of the FLC is nearly the same as the rate of convergence of the proportional controller. Furthermore, the performance of the parameter regulatory control can be characterized by a performance index called tracking error. Therefore, our proposed scheme can reduce transmission queuing delay and packet loss probability without causing the system to be unstable. The fuzzy rule base consists of a set of linguistic terms in the following form [16]:

$$R_i\ :\ \text{if } e \text{ is } U_i \text{ and } \Delta e \text{ is } V_i,\ \text{then } \mu \text{ is } W_i, \quad i = 1 \ldots m$$

where U_i and V_i are fuzzy subsets in their universe of discourse and W_i is a fuzzy singleton.

In our proposed scheme, 7 × 7 fuzzy rules are used, as listed in Table 1.

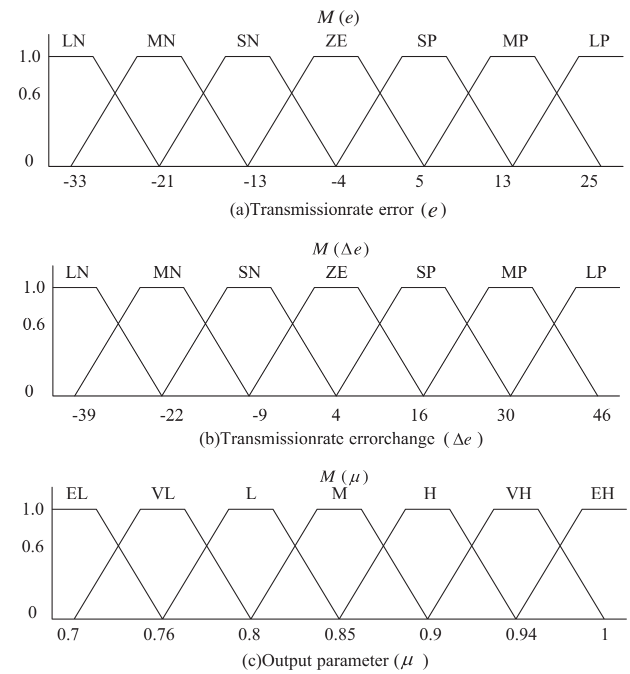

Fig. 6. Membership functions for the fuzzy set values.

From Fig. 4, the defuzzification output value μ is calculated by:

$$\mu = \frac{\sum_{i=1}^{n} u_i U_i}{\sum_{i=1}^{n} u_i} \tag{15}$$

4. Simulation results

In this section, we use NS2 to evaluate the results of the proposed model under different schemes. In Fig. 2, the simulation model has ten sensor nodes, one sink node and the BS. The transmission routing protocol of that model is a static routing transmission; the transmission data collected by sensor nodes are generated randomly and there are four types of traffic class: RT, HNRT, MNRT and LNRT. The traffic class has been set manually in advance by the sensor nodes. Table 2 shows the simulation parameters.

Table 1
Fuzzy rules.

		e						
		LN	MN	SN	ZE	SP	MP	LP
Δe	LN	EH	VH	H	M	M	L	M
	MN	EH	VH	H	M	M	M	EL
	SN	EH	VH	H	M	M	VL	EL
	ZE	EH	VH	H	M	L	VL	EL
	SP	EH	VH	M	M	L	VL	EL
	MP	EH	M	M	M	L	VL	EL
	LP	M	H	M	M	L	VL	EL

Table 2
Simulation parameters.

Network field	500 m × 500 m
Number of sensor nodes	10
Number of sink nodes	1
Packet size	500 bytes
Routing protocol	Static routing
Buffer size of sensor nodes	50 packets
Buffer size of sink nodes	100 packets
Simulation time/rounds	100 s/30 rounds

Table 3
The state of traffic classes in each sensor node.

Sensor node No.	RT ($W = 4$)	HNRT ($W = 3$)	MNRT ($W = 2$)	LNRT ($W = 1$)	P^i_{TRC}
Node 1	ON	ON	OFF	OFF	7
Node 2	OFF	ON	OFF	OFF	3
Node 3	ON	OFF	ON	OFF	6
Node 4	OFF	ON	ON	OFF	5
Node 5	ON	ON	OFF	OFF	7
Node 6	OFF	ON	ON	OFF	5
Node 7	OFF	ON	OFF	ON	4
Node 8	ON	ON	ON	ON	10
Node 9	OFF	OFF	OFF	ON	1
Node 10	ON	OFF	OFF	ON	5

Table 3 is a simulation: it is assumed that all the sensor nodes will collect the data from the four different traffic classes of which the weight values are four, three, two and one, respectively. Each node will be allocated a transmission rate according to the priority weight of the data transmission rate class. The transmission rate of each child node will be allocated by the sink node according to the weight of the data. In Fig. 2, we have calculated P^1_{TRC} of Node 1, which contains EF and LNRT traffic classes and is equal to 7. This is presented in Table 3.

We measure transmission rate for different nodes as shown in Fig. 7(a). In our proposed FTLP scheme with EWPBRC, we use FLC to regulate the TLP μ to obtain the optimum TLP and transmission rate for each node. Simulation results show TLP μ over rounds for Nodes 1–3 (Fig. 7(b)). Furthermore, we also calculate a new transmission rate for each node according to the TLP μ given. When the TLP is low, all parent nodes' transmission rates are high. When μ is increased, the transmission load in the network is also increased and the transmission rate for its child is high. Simulation results show that our proposed scheme adapts FLC to obtain the optimal TLP according to the mutual propagation of data sent from sensor nodes.

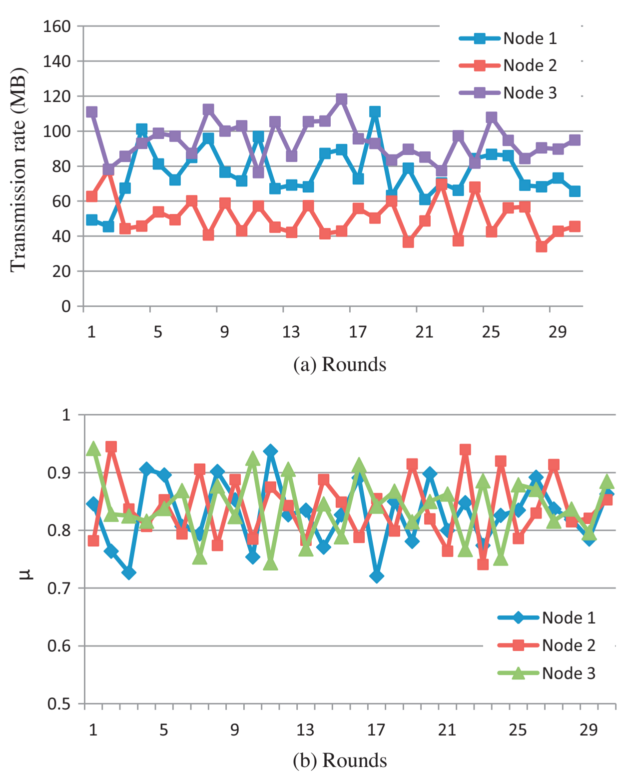

Fig. 7. (a) r^i_{in} total transmission rate for different nodes, (b) traffic load effect parameter μ over rounds for different nodes.

As shown in Figs. 8 and 9, we compare the performance of the EWPBRC scheme, that of the TLP scheme with EWPBRC and that of the FTLP scheme with EWPBRC, in terms of the average queuing delay and packet loss probabilities. The weighted value of the EWPBRC scheme is defined in Eq. (2) and the EWPBRC scheme without the TLP adjustment mechanism in sensor nodes. We simulate such that the TLP is $\mu = 0.9$ for the TLP scheme with EWPBRC and compare the FTLP scheme with EWPBRC in selecting optimal TLPs for sensor nodes.

In Fig. 8, we have evaluated the average queuing delays of the EWPBRC scheme, the TLP scheme using EWPBRC with $\mu = 0.9$ and the FTLP scheme with EWPBRC. In Fig. 8, the average queuing delays of the EWPBRC scheme, the TLP scheme using EWPBRC with $\mu = 0.9$ and the FTLP scheme with EWPBRC are: 0.3543 s, 0.3448 s and 0.3388 s, respectively. Because the EWPBRC cannot allocate transmission rates for sensor nodes when the traffic congestion increases, the TLP scheme with EWPBRC uses fixed TLP ($\mu = 0.9$) and cannot effectively distribute transmission rates among sensor

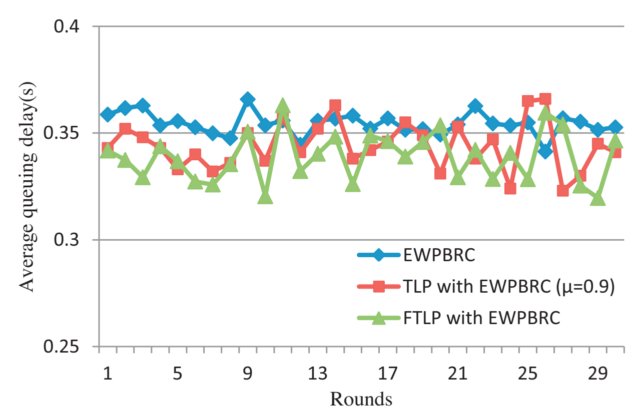

Fig. 8. Average queuing delay of all nodes over rounds for different schemes.

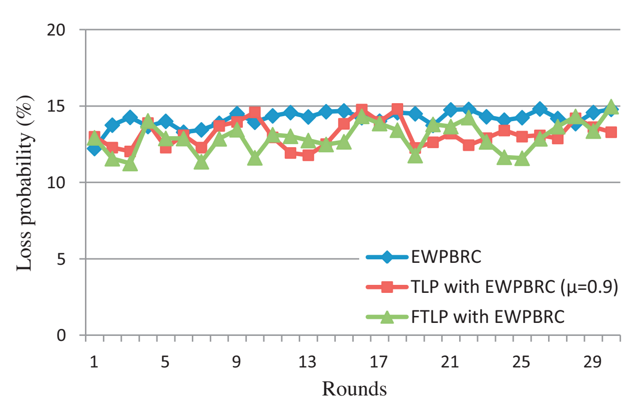

Fig. 9. Loss probability over rounds for different schemes.

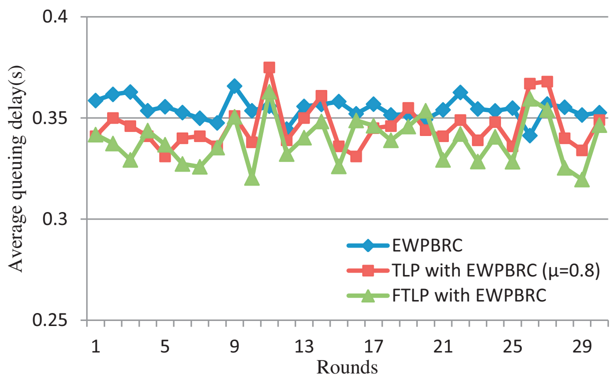

Fig. 10. Average queuing delay of all nodes over rounds for different schemes.

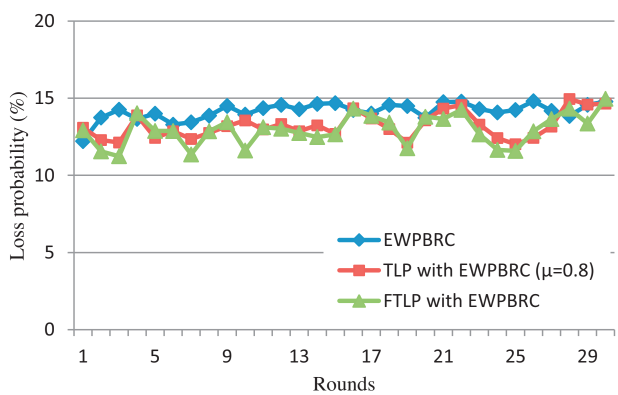

Fig. 11. Loss probability over rounds for different schemes.

nodes. Our proposed FTLP scheme with EWPBRC has the lowest average queuing delay and the EWPBRC scheme exhibits the highest average queuing delay.

In the transmission process, the transmission rate of each node is adjusted and Eq. (8) is used to allocate the new output transmission rate r_{out}^{k} to all the child nodes in order to mitigate packet loss. In Fig. 9, simulation results show that the average packet loss probabilities of the EWPBRC scheme, the TLP scheme using EWPBRC with $\mu = 0.9$ and the FTLP scheme with EWPBRC are: 14.16%, 13.15% and 12.96%, respectively. Notably, our proposed FTLP scheme with EWPBRC obtains the lowest packet loss probability.

To evaluate the effectiveness of the TLP scheme with EWPBRC with changes in TLP $\mu = 0.8$, we performed another simulation, as shown in Figs. 10 and 11. In Fig. 10, we compared the average queuing delay time of three schemes: the EWPBRC scheme, the TLP scheme using EWPBRC with $\mu = 0.8$ and the FTLP scheme with EWPBRC. The simulation results show that the average queuing delays of the fixed-rate PBRC scheme, the TLP scheme which uses EWPBRC with $\mu = 0.8$ and the FTLP scheme with EWPBRC are: 0.3543 s, 0.3456 and 0.3388 s, respectively. Our FTLP scheme with EWPBRC exhibits the shortest time, while the EWPBRC scheme results in the longest average queuing delay, as described in Fig. 10.

We compared the average packet loss probability of the EWPBRC scheme, the TLP scheme using EWPBRC with $\mu = 0.8$ and the FTLP scheme with EWPBRC in Fig. 11. Fig. 11 shows that the average packet loss probabilities of the EWPBRC scheme, the TLP scheme using EWPBRC with $\mu = 0.8$ and the FTLP scheme with EWPBRC are: 14.16%, 13.22% and 12.96%, respectively. From Figs. 10 and 11, our proposed FTLP scheme with EWPBRC has the lowest packet loss probability because our proposed FTLP scheme with EWPBRC uses FLC to obtain the optimum μ.

In next simulation, we adjust some simulation parameters based on [13] to be shown in Table 5; the transmission data is collected by sensor nodes which are default generator and traffic classer the same previous simulation.

In this scenario, for sensor node 1 which has all traffic classes, P_{TRC}^{1} is equal to 20, while for sensor node 10 which has only RT and MNRT traffic classes, the traffic class priority, P_{TRC}^{10} is equal to 4. The P_{TRC}^{i} of each sensor node is given in Table 6.

In this simulation, we regulate the TLP μ to obtain the optimum TLP and transmission rate for each node by FLC, according to transmission rate of sensor nodes that it is shown in Fig. 12(a). In addition, we calculate a new transmission rate for each node according to the TLP μ. Simulation results show TLP μ over rounds for Nodes 1–3 in Fig. 12(b).

Fig. 13 shows the average queuing delay of all nodes over rounds of the EWPBRC scheme, the TLP scheme using EWPBRC with $\mu = 0.9$, EWPBRC with $\mu = 0.8$ and the FTLP scheme with EWPBRC. The average queuing delays of the EWPBRC scheme, the TLP scheme using EWPBRC with $\mu = 0.9$ and the FTLP scheme with EWPBRC

Table 4
Performance of simulation.

Different schemes	Average delay (s)	Average loss probability (%)
EWPBRC	0.3913	14.74
FTLP with EWPBRC	0.3388	12.96
TLP with EWPBRC ($\mu = 1$)	0.3448	13.29
TLP with EWPBRC ($\mu = 0.9$)	0.3440	13.15
TLP with EWPBRC ($\mu = 0.8$)	0.3453	13.26
TLP with EWPBRC ($\mu = 0.7$)	0.3461	13.32

Table 5
Simulation parameters.

Network field	500 m × 500 m
Number of sensor nodes	10
Number of sink nodes	1
Packet size	250 bytes
Routing protocol	Static routing
Buffer size of sensor nodes	100 packets
Buffer size of sink nodes	100 packets
Simulation time/rounds	100 s/30 rounds

Table 6
The state of traffic classes in each sensor node.

Sensor Node No.	RT ($W = 10$)	HNRT ($W = 6$)	MNRT ($W = 3$)	LNRT ($W = 1$)	P_{TRC}^{i}
Node 1	ON	ON	ON	ON	20
Node 2	ON	ON	ON	OFF	19
Node 3	ON	ON	OFF	ON	17
Node 4	ON	ON	OFF	OFF	16
Node 5	ON	OFF	ON	ON	14
Node 6	ON	OFF	ON	OFF	13
Node 7	ON	OFF	OFF	ON	11
Node 8	OFF	ON	ON	ON	10
Node 9	OFF	ON	ON	OFF	9
Node 10	OFF	ON	OFF	ON	7

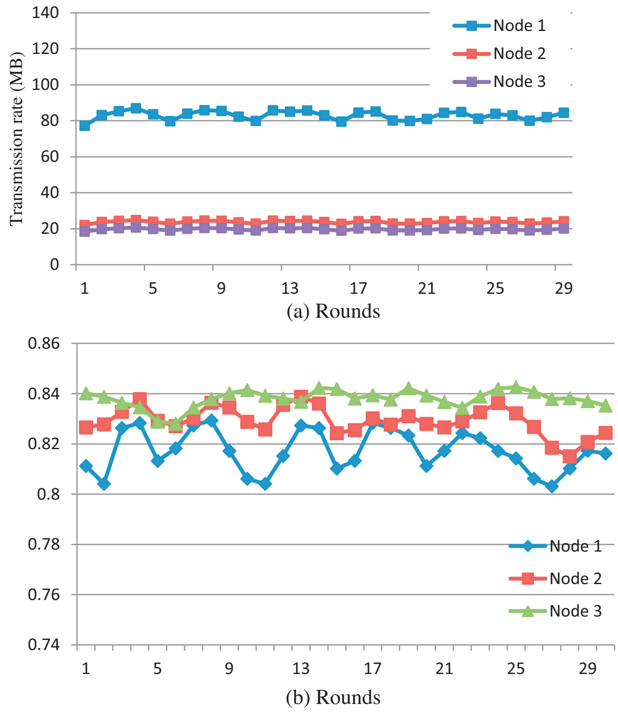

Fig. 12. (a) r_{in}^{i} total transmission rate for all the parent nodes, (b) traffic load effect parameter μ over rounds for different nodes.

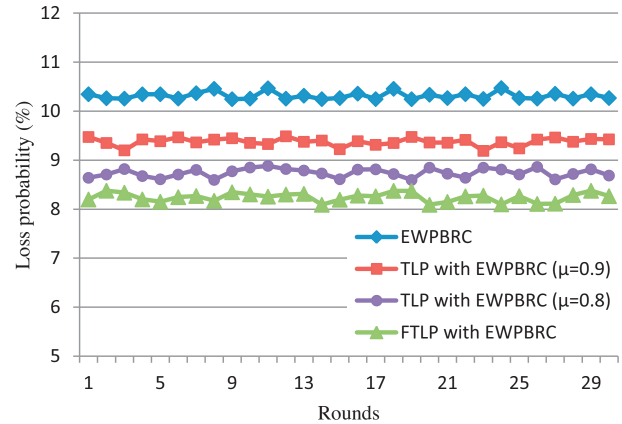

Fig. 14. Loss probability over rounds for different schemes.

Table 7
Performance of simulation.

Different schemes	Average delay (s)	Average loss probability (%)
EWPBRC	0.3348	10.32
FTLP with EWPBRC	0.3257	8.24
TLP with EWPBRC ($\mu = 1$)	0.3328	9.96
TLP with EWPBRC ($\mu = 0.9$)	0.3299	9.36
TLP with EWPBRC ($\mu = 0.8$)	0.3275	8.75
TLP with EWPBRC ($\mu = 0.7$)	0.3336	9.99

are: 0.3348 s, 0.3299 s, 0.3275 s and 0.3257 s, respectively. Our proposed FTLP scheme with EWPBRC such that FLC can regulate TLP and control the output transmission rate of each node so as to obtain the lowest average queuing delay. However, the EWPBRC scheme cannot allocate transmission rates for sensor nodes when the traffic congestion increases for the reason that exhibits the highest average queuing delay.

In Fig. 14, depicts the loss probability over rounds by EWPBRC scheme, the TLP scheme using EWPBRC with $\mu = 0.9$, EWPBRC with $\mu = 0.8$ and the FTLP scheme with EWPBRC. Simulation results show that the average packet loss probabilities are: 10.32%, 9.36%, 8.75% and 8.24%, respectively. Obviously, our proposed FTLP scheme with EWPBRC obtains the lowest packet loss probability. This is because our purpose scheme to achieve the optimal traffic load parameter for transmission rate distribution on sensor nodes.

In all previous simulations, the proposed FTLP scheme with EWPBRC can regulate TLPs effectively. The proposed model

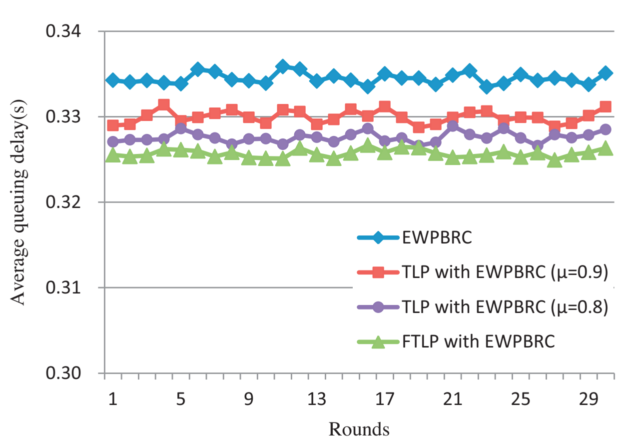

Fig. 13. Average queuing delay of all nodes over rounds for different schemes.

can support transmission data through random generation. We evaluated the performance of the proposed FTLP scheme with EWPBRC under different conditions and with different schemes. The simulation results show that FTLP scheme with EWPBRC can achieve a low average queuing delay and low packet loss probability.

In Tables 4 and 7, we compared the performance of the EWPBRC scheme and the TLP scheme with EWPBRC with that of the FTLP scheme with EWPBRC, where the TLP scheme with EWPBRC has four parameters: 1, 0.9, 0.8 and 0.7. Tables 4 and 7 show that the performance of the FTLP scheme with EWPBRC outperforms that of the EWPBRC and the TLP scheme with EWPBRC in terms of average queuing delay and average loss probability.

5. Conclusions

This paper proposes a new scheme combining EWPBRC with FLC TLPs (FTLP) for improving transmission performance in WMSNs. Notably, our scheme selects the appropriate TLP μ for estimating the optimal transmission rate. In the transmission period, our proposed FTLP scheme with EWPBRC uses an FLC to infer a suitable TLP μ for each sensor node in order to allocate transmission rate. The simulation results show that our proposed schemes have outperformed the EWPBRC and the TLP scheme with EWPBRC in terms of average queuing delay and average loss probability. By mitigating congestion, improving upon packet loss probability and reducing average queuing delay, the proposed scheme meets the QoS requirements for network transmission.

Acknowledgements

This work was supported in part by the National Science Council (NSC) of Republic of China under grant No. NSC 102-2221-E-025-001.

References

[1] J. Ben-Othman, B. Yahya, Energy efficient and QoS based routing protocol for wireless sensor network, Journal of Parallel and Distributed Computing 70 (8) (2010) 849–857.

[2] I.F. Akyildiz, T. Melodia, K.R. Chowdhury, A survey on wireless multimedia sensor networks, Computer Networks 51 (4) (2007) 921–960.

[3] B. Yahya, J. Ben-Othman, Towards a classification of energy aware MAC protocols for wireless sensor networks, Journal of Wireless Communications and Mobile Computing 9 (12) (2009) 1572–1607.

[4] S. Floyd, V. Jacobson, Random early detection gateways for congestion avoidance, IEEE/ACM Transactions on Networking 1 (4) (1993) 397–413.

[5] C. Wang, K. Sohraby, M. Daneshmand, Y. Hu, Upstream congestion control in wireless sensor networks through cross-layer optimization, IEEE Journal on Selected Areas in Communications 5 (4) (2007) 786–795.

[6] K. Nichols, V. Jacobson, L. Zhang, A two-bit differentiated services architecture for the internet, IETF RFC 2638 (1999).

[7] I. Chamodrakas, D. Martakos, A utility-based fuzzy TOPSIS method for energy efficient network selection in heterogeneous wireless networks, Applied Soft Computing 11 (4) (2011) 3734–3743.

[8] Y.L. Chen, C.P. Li, J.W. Wang, J.H. Wen, Performance analysis of multi-step power control algorithm for cellular systems, European Transactions on Telecommunications 19 (2) (2011) 151–167.

[9] Y.L. Chen, Y.S. Lin, J.W. Wang, J.H. Wen, Adaptive fuzzy rate management and power control for in multimedia CDMA cellular systems, Computer Communication 31 (10) (2008) 1901–1910.

[10] Y.L. Chen, Y.S. Lin, J.W. Wang, J.H. Wen, Combined fuzzy-based power control with window-based transmission rate management in multimedia CDMA cellular systems, International Journal of Electronics and Communications 65 (4) (2011) 377–383.

[11] P.R. Chang, B.C. Wang, Adaptive fuzzy power control for CDMA mobile radio system, IEEE Transaction on Vehicular Technology 45 (2) (1996) 225–236.

[12] P.R. Chang, B.C. Wang, Adaptive fuzzy proportional integral power control for a cellular CDMA system with time delay, IEEE Journal on Selected Areas in Communications 14 (9) (1996) 1818–1829.

[13] M.H. Yaghmaee, D.A. Adjeroh, Priority-based rate control for service differentiation and congestion control in wireless multimedia sensor networks, Computer Networks 53 (11) (2009) 1798–1811.

[14] N.C. Wang, Y.F. Huang, W.L. Liu, An improved transport protocol for mobile Ad Hoc networks with fuzzy logic control, Journal of Internet Technology 10 (3) (2009) 229–236.

[15] H.X. Li, H.B. Gatland, A new methodology for designing a fuzzy logic controller, IEEE Transactions on Systems Man and Cybernetics 25 (3) (1995) 505–512.

[16] C. Elmas, O. Deperlioglu, H.H. Sayan, Adaptive fuzzy logic controller for DC–DC converters, Expert Systems with Applications 36 (2) (2009) 1540–1548.